Chapter 1

Imaging Functional Nucleic Acid Delivery to Skin

Roger L. Kaspar, Robyn P. Hickerson, Emilio González-González, Manuel A. Flores, Tycho P. Speaker, Faye A. Rogers, Leonard M. Milstone, and Christopher H. Contag

Abstract

Monogenic skin diseases arise from well-defined single gene mutations, and in some cases a single point mutation. As the target cells are superficial, these diseases are ideally suited for treatment by nucleic acid-based therapies as well as monitoring through a variety of noninvasive imaging technologies. Despite the accessibility of the skin, there remain formidable barriers for functional delivery of nucleic acids to the target cells within the dermis and epidermis. These barriers include the stratum corneum and the layered structure of the skin, as well as more locally, the cellular, endosomal and nuclear membranes. A wide range of technologies for traversing these barriers has been described and moderate success has been reported for several approaches. The lessons learned from these studies include the need for combinations of approaches to facilitate nucleic acid delivery across these skin barriers and then functional delivery across the cellular and nuclear membranes for expression (e.g., reporter genes, DNA oligonucleotides or shRNA) or into the cytoplasm for regulation (e.g., siRNA, miRNA, antisense oligos). The tools for topical delivery that have been evaluated include chemical, physical and electrical methods, and the development and testing of each of these approaches has been greatly enabled by imaging tools. These techniques allow delivery and real time monitoring of reporter genes, therapeutic nucleic acids and also triplex nucleic acids for gene editing. Optical imaging is comprised of a number of modalities based on properties of light-tissue interaction (e.g., scattering, autofluorescence, and reflectance), the interaction of light with specific molecules (e.g., absorbtion, fluorescence), or enzymatic reactions that produce light (bioluminescence). Optical imaging technologies operate over a range of scales from macroscopic to microscopic and if necessary, nanoscopic, and thus can be used to assess nucleic acid delivery to organs, regions, cells and even subcellular structures. Here we describe the animal models, reporter genes, imaging approaches and general strategies for delivery of nucleic acids to cells in the skin for local expression (e.g., plasmid DNA) or gene silencing (e.g., siRNA) with the intent of developing nucleic acid-based therapies to treat diseases of the skin.

Key words siRNA, Topical delivery, Nucleic acid, Skin, Monogenic, Pachyonychia congenita, Optical imaging, Biophotonic, Bioluminescence, Fluorescence, Keratin, GFP, Genetherapy

1 Introduction

Delivery of nucleic acids to cells in culture has been routine in biology laboratories for over 30 years, and has enabled thorough studies of gene expression and regulation in single cells and in

Zdravka Medarova (ed.), *RNA Imaging: Methods and Protocols*, Methods in Molecular Biology, vol. 1372,
DOI 10.1007/978-1-4939-3148-4_1,

populations of cultured cells. These delivery tools have been modified, and in some cases optimized, for delivery of specific lengths, or composition, of nucleic acids even to primary cells taken directly from animals or humans. Nucleic acid transfer to cells can be accomplished by physical methods (e.g., electroporation, microinjection, ultrasound, and laserfection) that transiently compromise the barriers, or via chemical methods that integrate nucleic acid such as incorporation into liposomes, nanoparticles, cationic polymers, dendrimers, and magnetic beads. Alternatively, chemical modifications of the nucleic acid that create self-delivery nucleic acids, or viral vectors that target cells of the skin, could be used. Physical methods may be needed to overcome the tissue barriers and it may be necessary to combine methods to both cross the tissue barriers and traverse cellular membranes [1]. Self-delivery nucleic acids have been described that confer reasonable cellular uptake in the absence of transfection reagents in cultured cells [2]. Yet nucleic acid transfer to cells in the complex environments of tissues and organs has not been as facile, and the broad potential of using nucleic acids to treat human disease is still in its infancy. Naturally occurring physical and biochemical barriers have been selected through evolution to prevent transfer of genetic material from the environment into the organs, tissues and cells of our bodies, and these comprise the primary challenge to the effective development of nucleic acid-based therapies to treat human disease.

Among the diseases that could be treated with nucleic acids, monogenic skin diseases offer unique opportunities to develop new tools with potential for clinical impact [3–5]. The skin is an accessible organ and the single gene target in monogenic diseases simplifies the requirements for the therapeutic nucleic acid [6]. We have been developing nucleic acid therapeutics to treat the rare inherited skin disease, pachyonychia congenita (PC) [4, 7]. This keratinization disorder is a result of dominant mutations, including single nucleotide changes, in one of the inducible keratin genes, resulting in aberrant intermediate filament formation. The dominant nature of the mutation, coupled with the apparent redundancy of keratins (i.e., selective inhibition of the mutant keratin preserves wild type expression and the lowered amount can be compensated by other keratins [8, 9]) and the apparent ability to achieve a therapeutic effect when only 50 % inhibition of mutant keratin expression achieved [10, 11], make this and similar keratin disorders ideal for siRNA therapeutics. However, our experience confirms that of others, that it is extremely difficult to get biologically active nucleic acids into epidermal cells at therapeutically relevant levels.

Nucleic acid–based vaccines have been developed using skin delivery and are being considered for clinical use [12–14]. Moreover, the fact that there is an amplification through transcription and translation and potentially more engagement of the immune

response through the frontline skin immune defenses including Langerhans and dendritic cells, this application tolerates inefficient delivery. Delivery of therapeutically relevant levels of siRNA to a significant number of cells in the skin presents significant challenges over what can be done with nucleic acid based vaccines. We have demonstrated effective gene silencing of the keratin target gene in cultured cells, human skin equivalents and also in a limited clinical study using multiple injections into affected areas of the foot [2, 4, 7]. The fact that we observed partial resolution of the PC lesion injected with mutant-specific siRNA suggests that injections do deliver nucleic acids to epidermal cells and indicates that skin delivery is feasible; however, the injections are inefficient and the delivery is likely facilitated by the pressure generated, exacerbating the associated pain to a clinically unacceptable level [15]. We have attempted to overcome this obstacle using a variety of delivery tools and comparing and combining delivery technologies in mouse models. Here we summarize the lessons learned and the advances to date. Despite the advances by us and many others in this field, nucleic acid delivery remains a major hurdle to the development of effective nucleic acid therapeutics for skin.

We reasoned that we could further advance this field by developing and using imaging technologies that would enable visualization of delivery of the therapeutic, or mimics of the therapeutic, as a means of improving nucleic acid transfer. We further reasoned that if we linked the therapeutic target to expression of optical reporter genes, we could also visualize effective, and in many cases ineffective, delivery of the therapeutic nucleic acid to the target cells in the skin [16]. Here we summarize these technologies as well as the imaging tools available for assessing nucleic acid delivery with a focus on the skin applications.

1.1 Problem and Possible Solution: Monogenic Skin Diseases and siRNA as a Therapeutic Strategy

Pachyonychia congenita is a dominant negative monogenic skin disorder caused by mutations, including single nucleotide mutations, in the inducible keratin genes encoding K6a, K6b, K16, and K17, resulting in dystrophic nails and exquisitely painful palmoplantar keratoderma [17, 18]. An siRNA has been developed that has the ability to target the K6a N171K single nt mutation with little or no effect on wild type expression [3, 7]. This siRNA has been successfully evaluated in a small clinical trial in which injected siRNA resulted in localized keratoderma clearing and reduction of pain [4]. Unfortunately, the mode of administration, intralesional injection, was unacceptably painful and required oral pain medications and a regional pain block. PC is one of many rare dominant negative skin disorders with unmet clinical needs (largely due to small patient populations and the reluctance of the pharmaceutical industry to develop small molecule inhibitors for small markets) [19], which could benefit from development of a patient-friendly siRNA delivery platform. Specific and potent siRNA agents are the most promising therapeutics for this class of skin disorders [3].

1.2 Imaging Nucleic Acid Delivery and Function to Accelerate Development of Therapeutics

Given the large number of variables associated with effective delivery of functional nucleic acids to the skin, tools that enable visualization of each step in the process would have tremendous benefit in the optimization process. Therefore, we have spent time developing, and using, tools to enable imaging delivery of the therapeutic, assessing distribution in the tissue and determining the effects on the genetic target. These tools are largely based on imaging of optically active dyes and proteins over a range of scales from macroscopic to microscopic imaging (Table 1). Optical imaging offers the potential to multiplex the analysis such that the therapeutic can be imaged with one optical signature and the expression of the target gene with a separate optical feature. The devices are typically able to collect a reference image of the anatomy—either macroscopic or microscopic—and an image of the optical marker can be superimposed on this image for reference. Since the background is typically shown in black and white we refer to these images as gray-scale reference images.

In vivo bioluminescence imaging was developed for the purpose of enabling the study of biological processes in the context of organs and tissues of living subjects where the contextual influences remain intact and has been applied to imaging of infection, cancer, stem cell biology and many other biological processes [25]. The basis of this preclinical imaging modality is a class of light emitting enzymes call luciferases that are used as reporters of biological function [25]. In vivo bioluminescence imaging has been used to assess nucleic acid delivery to many different organ systems in small animal models. Optical imaging tools can image over a range of scales such that nucleic acid delivery can be assessed at the level of the organ or the cell in vivo and then validated using the

Table 1
In vivo optical imaging tools to assess gene delivery to skin

	Mode(s)	Imaging scale	Status of clinical approval	References
Cell-vizio	Fluorescence	Microscopic	Approved for GI and in clinical use	[20]
Dual-axis microscope	Fluorescence	Microscopic	Tested in humans for GI cancer and in dermatology	[21]
Caliber ID VivaScope	Fluorescence and reflectance	Microscopic	In clinical use in dermatology	[16, 22, 23]
Dermatoscope	Fluorescence, polarized light, and reflectance	Microscopic	In clinical use in dermatology	[24]
IVIS	Wide-field fluorescence and bioluminescence	Macroscopic	Preclinical device for a variety of organ systems	[5, 7, 9]

same optical tags in excised organs. Once excised, the tissue can be subjected to a multitude of imaging and molecular assays to validate the in vivo image and multiplex the analysis.

There are a number of architectures of confocal microscopes that vary with illumination and collection paths (Fig. 1) and one of these uses a dual axis architecture that increases signal to noise and

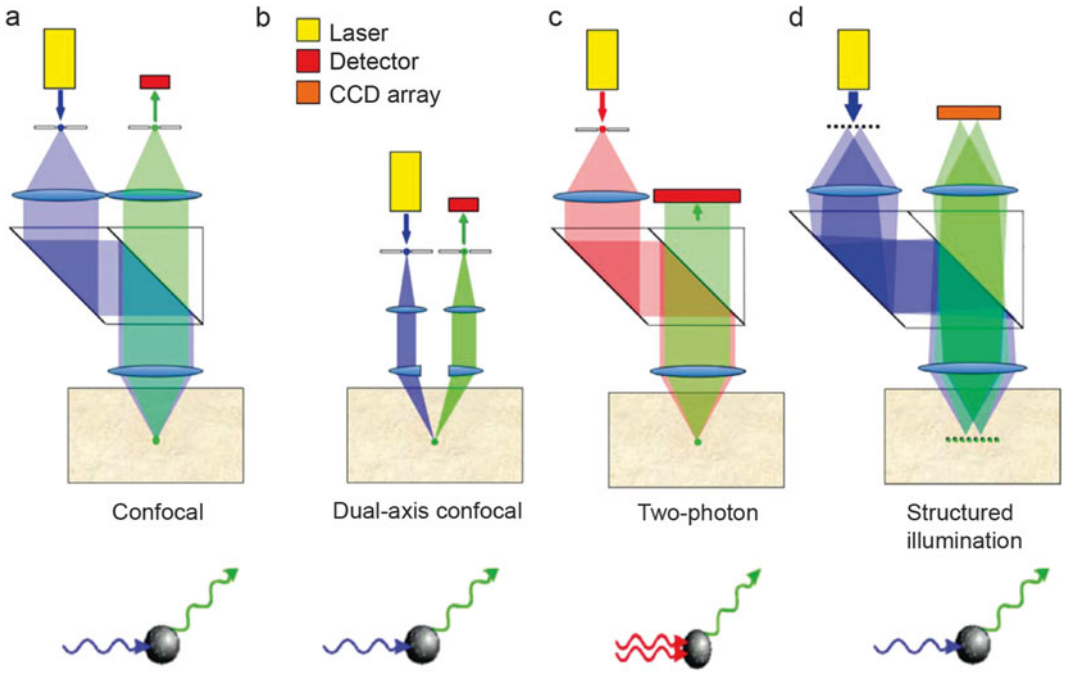

Fig. 1 Microscope designs. (**a**) The conventional confocal microscope, using a high-NA (0.8–1.4) objective and two pinholes to provide a point source and point detector (figure and text from Liu et al. [57, 58]). Images are collected by scanning the focal spot within the specimen in either reflectance or fluorescence (shown) modes. Excitation light (*blue*) is absorbed by the fluorescent molecules in the specimen and fluorescence emission (*green*) is collected by the point detector. (**b**) The dual-axis confocal microscope, using two low-NA (0.1–0.2) objective lenses and two pinholes to provide a point source and point detector. The excitation (*blue*) and emission (*green*) beams are spatially separated within the specimen, except where they overlap at the focus. (**c**) The multiphoton microscope using a high-NA (0.8–1.4) objective and a single pinhole to provide a point source. The *red* beam represents the long-wavelength excitation light (high-peak-power pulsed laser), which is nonlinearly absorbed by the fluorescent molecules in the specimen. The efficiency of two-photon absorption, for example, scales as the square of the intensity of the light, and is therefore confined to just the focus of the excitation beam. The *green* beam represents the shorter-wavelength fluorescence emission light collected by a large area detector. (**d**) The structured illumination microscope can be used to gather full-field (single-shot) 2-D images by a photodetector array (CCD) in either reflectance or fluorescence (shown) modes. The images are quasi-optically sectioned due to the fact that the structured pattern is only imaged with high contrast at the focal plane within the specimen. By spatially modulating the illumination pattern, out-of-focus (low-contrast) light may be distinguished from, and digitally filtered away from the in-focus light that is modulated with high contrast. The multiple *blue* beams represent a pattern of excitation light beams emanating from a structured light source, which is absorbed by the fluorescent molecules in the specimen. The respective green beams represent the fluorescence emission light collected by the CCD

enables radical miniaturization [26–29]. Handheld microscopes of this type were used to assess effective delivery of siRNA to the skin of mice and humans [21, 30]. The core of these miniature microscopes are microelectromechanical systems (MEMS) scanners [31] that can enable 2-D *en face* imaging at four frames per second. Three-dimensional images can also be acquired by translating the MEMS scanner in the depth direction with a piezoelectric actuator to sequentially save image stacks. This tool was initially developed for imaging in the gastrointestinal tract [32], but its potential in dermatology was recognized early in its development [26].

1.3 In Vivo Microscopy with the VivaScope 2500

The VivaScope is based on a standard confocal architecture but has been designed for in vivo use—both clinical and preclinical versions are available. Anesthetized mice can be analyzed with a modified Caliber ID VivaScope 2500 [22, 33] that has been upgraded for dual fluorescence capabilities with a blue (488 nm) and a post-manufacture addition of a green (532 nm) laser [16, 34] (Fig. 1). Briefly, *z*-stacks of images are acquired at successive 1.6 μm *z*-depths using native VivaScan software (v. VS008.01.09) and post-processed using public domain Fiji java-based image processing software [35]. Reflectance images are acquired using the 658 nm laser source with an "open" emission window. Sequential fluorescent images can be acquired using the 488 nm and 532 nm excitation laser and with the 531 and 607 nm emission filters, respectively. Figure 2 shows an example of visualizing EGFP and tdTFP following delivery of EGFP and tdTFP expression plasmids to mouse footpad skin. To increase the effective resolution of the VivaScope images, ten nominal images can be taken at each *z*-step and averaged to produce a more refined image. Because in vivo imaging is influenced by respiration and other minor subject motion, successive frames can be co-registered using an affine transform [36] (distributed with Fiji software as the StackReg plugin) prior to any frame-averaging. Images can be further intensity-scaled to maximize contrast with the Fiji software.

1.4 Evaluating siRNA Therapeutics Using Transgenic Reporter Mice with Optical Readouts

There was a need to develop a transgenic reporter mouse to enable in vivo bioluminescence imaging and fluorescence imaging of effective delivery of functional siRNA to cells in the skin along with the tools to look at the tissue microstructure (Figs. 3 and 4). The reporter transgenes in these animals were used to visualize gene silencing. To generate such a mouse, we crossed a Cre-expressing transgenic mouse with a multifunctional reporter mouse [33]. The construct in the multifunctional reporter mouse consisted of a click beetle luciferase and GFP gene fusion (CBL/hMGFP) cassette from the pCBL/hMGFP vector inserted downstream of Renilla luciferase (rLuc), with the two genes separated by a strong translation stop sequence in the following order, loxP-rLuc-stop-loxP-CBL-hMGFP. This construct, called RLG, was used to

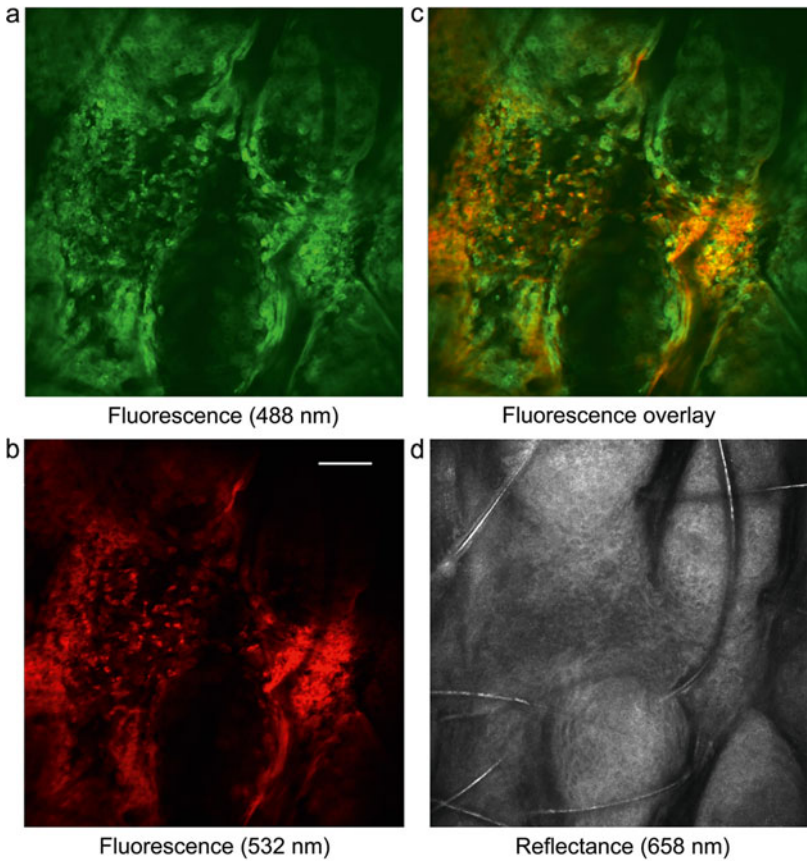

Fig. 2 Noninvasive subcellular imaging of EGFP and tdTFP expression in mouse footpad. EGFP/wt K6a (pTD241) and tdTFP/mut K6a (pTD203) UBC promoter expression plasmids (11 μg of each) were co-injected intradermally into a mouse footpad. At 36 h after injection, the footpad of the living mouse was noninvasively imaged for fluorescence using a modified Caliber ID VivaScope 2500 using 488 nm (EGFP, panel (**a**)) and 532 nm (tdTFP, panel (**b**) as well as overlay, panel (**c**)) lasers as well as with a 658 nm laser (reflectance) to determine depth and general skin structure (panel (**d**)). A z-stack of images (1.6 μM intervals) was acquired sequentially with each laser. The selected images shown from the z-stack are at 50-μm depth. Scale bar = 100 μM. A similar imaging procedure with keratin 6a (mutant and wild type)/reporter expression plasmids was used to noninvasively monitor the functional delivery and effectiveness of an siRNA specific to the keratin 6a N171K mutation that causes pachyonychia congenita [16]. Note the absence of EGFP expression in the nuclei

generate the transgenic skin reporter mouse using standard methods of pronuclear injection. The RLG transgene contains the CAG (CMV enhancer-chick β-actin) promoter [37], the coding sequence of rLuc (flanked by loxP sites) and the coding sequence of CBL fused to hMGFP. This transgenic mouse was crossed with a Tg(Krt14-cre)1Amc transgenic mouse (The Jackson Laboratory, Bar Harbor, ME) expressing Cre recombinase driven by the keratinocyte-specific K14 promoter with the intent of generating a mouse with the fusion reporter, CBL-hMGFP, expressed in keratinocytes. The use of a gene fusion containing a luciferase (CBL)

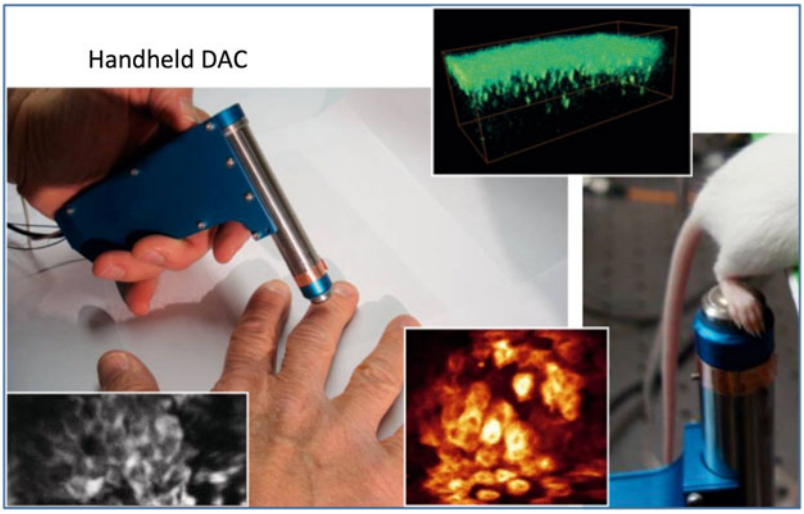

Fig. 3 DAC microscope imaging of the skin. One version of the DAC microscope is a hand-held device designed for skin imaging, and it has been used for imaging the effects of siRNA on GFP expression in the skin [21] and to image skin microanatomy. Stepping in the *z* direction is done with a piezo motor in the handle of the microscope and the *x*–*y* scan is performed with a MEMS scan mirror. The histology images are of human skin (*lower left*), GFP expression (*upper right*), and mouse skin (*lower right*)

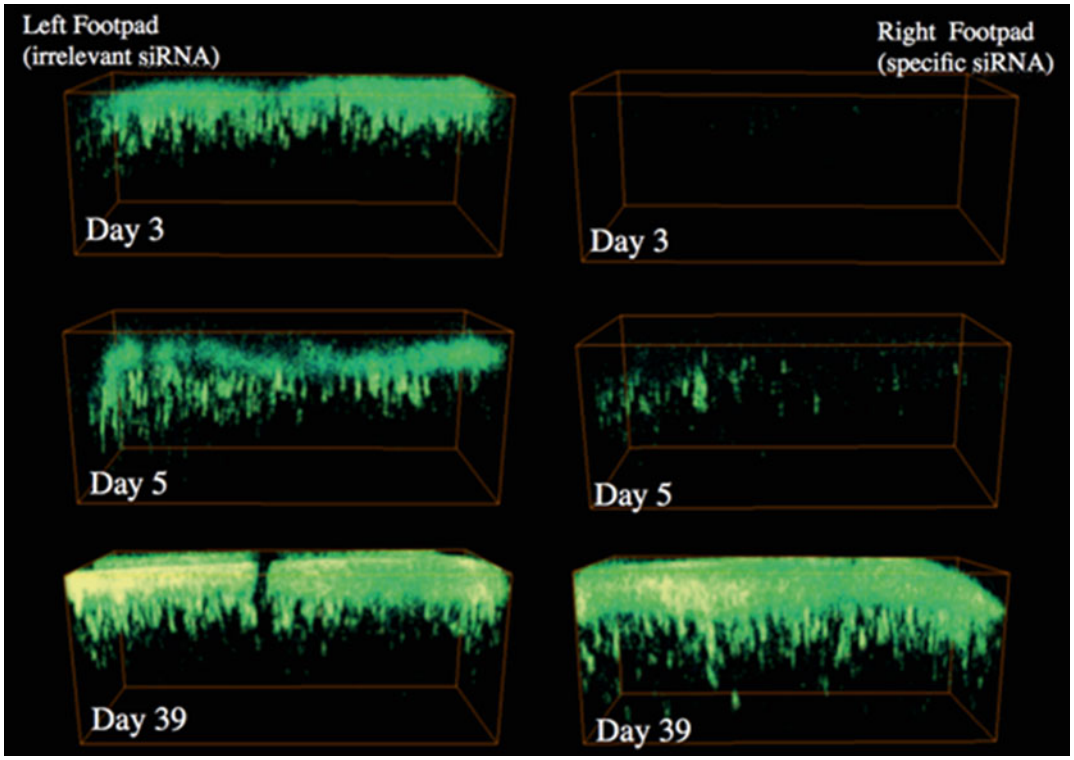

Fig. 4 Visualizing the effects of siRNA on GFP expression in the skin. Transgenic reporter mice were treated with either irrelevant siRNA (*left*) or siRNA directed at the GFP transcript (*right*) and imaged over time using a DAC microscope. The specific siRNA resulted in gene knockdown at day 3 and 5 and restoration of expression is apparent at day 39 [21]

and a fluorescent protein (hMGFP) allows use of a single siRNA (CBL3 siRNA) to silence both markers, enabling multimodal imaging of gene silencing. Mice resulting from this cross were tested for the expression of CBL by bioluminescence imaging in an IVIS 200 Imaging System after intraperitoneal injection of luciferin (30 mg/kg body weight). To improve optical imaging analyses, Tg CBL/hMGFP mice were bred with Balb/c mice (a white strain) in order to obtain a white background to facilitate in vivo detection of hMGFP signal using confocal microscopy. Subsequently, the CBL/hMGFP mice were crossed with skh1 hairless mice to enable experiments to be performed on the back of the mice using topical formulations and microneedle devices without interference of the autofluorescence and scatter from the hair. GFP expression in the skin of this mouse was validated using frozen sections [33] and then used to evaluate delivery of siRNA targeting the reporter construct (CBL3 siRNA) by looking for silencing of luciferase and/or GFP expression using either macroscopic or microscopic imaging [33, 34, 38, 39].

Treatment of some skin diseases will require long-term genetic modifications to correct mutations. Epidermal gene editing has been enabled by advances in nucleic acid biochemistry, and these strategies require that editing molecules reach keratinocyte nuclei. We have employed fluorescently tagged molecules that form triplexes with chromosomal *supFG1* DNA to monitor transfer into cell nuclei in the skin [23]. These studies demonstrated that a deoxyoligonucleotide, FITC-AG30, accumulated in keratinocyte nuclei after topical application to stratum corneum-stripped skin (Fig. 5) or intradermal injection [23]. Similarly, a clamp-forming peptide-nucleic acid conjugated to the transduction peptide antennapedia, FITC-PNA-Antp, accumulated in epidermal keratinocyte nuclei after intradermal injection (Fig. 5) [23]. Most critically, we have demonstrated that these triplex forming molecules induce sequence-specific modifications in epidermal DNA in a *supFG1* transgene after intradermal or intraperitoneal injection [23].

1.5 Technologies for Nucleic Acid Delivery

A number of technologies, including chemical and mechanical, have been developed and evaluated for nucleic acid skin delivery (Table 2). Beginning in 2008, we were part of an NIH-funded consortium formed to develop validated systems to evaluate methodologies for nucleic acid delivery including siRNAs [22, 40]. As part of this consortium, a number of delivery technologies were evaluated using the Tg CBL/hMGFP mouse reporter skin model in which a dual reporter consisting of Monster GFP (hMGFP) and click beetle luciferase (CBL) is expressed in the epidermis [33]. This model had previously been utilized to demonstrate that dissolvable microneedles, manufactured with polyvinyl alcohol (PVA) and loaded with a target-specific self-delivery siRNA cargo, were able to inhibit reporter expression in mouse footpad skin

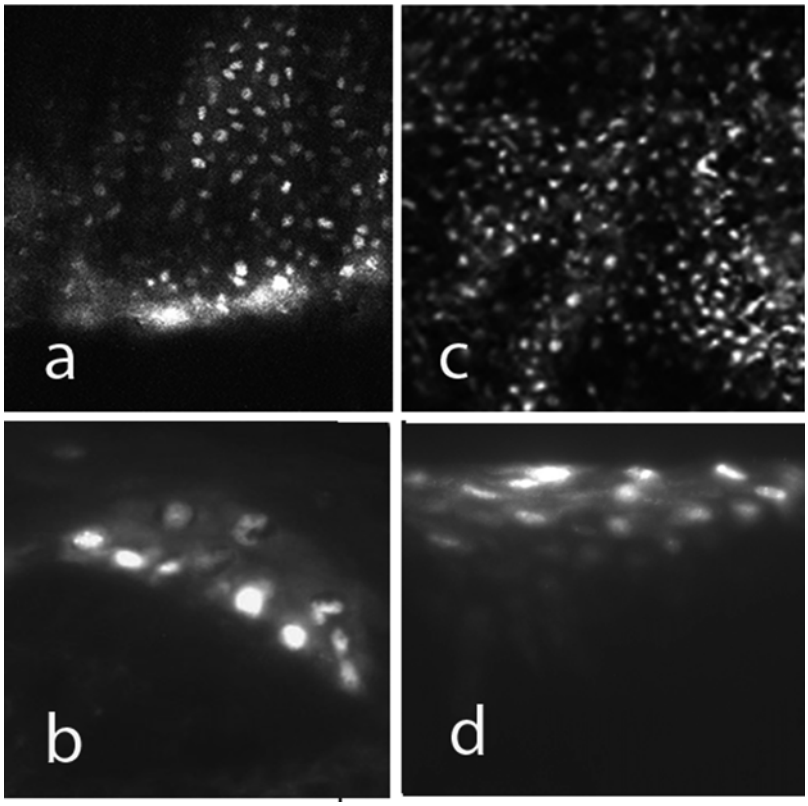

Fig. 5 FITC-tagged triplex forming molecules (TFM) accumulate in keratinocyte nuclei [23]. Fluorescent TFM capable of initiating editing of chromosomal DNA were delivered to the skin of mice. These mice had a *supFG1* transgene. The peptide nucleic acid (PNA) and the single-stranded deoxyoligonucleotide (AG30) had previously been shown to form triplex structures with the *supFG1*. Each molecule was conjugated to FITC for imaging, and the PNA was conjugated to antennapedia peptide (Antp) to facilitate delivery across membranes. After 1–2 h, live skin was imaged *en face* using the VivaScope 2500 in fluorescence mode, and then vertical sections of frozen skin samples were viewed by epifluorescence microscopy. (**a**) *En face* confocal fluorescence image of tail epidermis 2 h after intradermal injection of FITC-PNA-Antp. (**b**) Vertical section through epidermis showing FITC-PNA-Antp in nuclei of all epidermal layers. (**c**) *En Face* confocal fluorescence image of epidermis 1 h after application of aqueous buffer of FITC-AG30 to stratum corneum-stripped back skin. (**d**) Vertical section through epidermis showing FITC-AG30 in nuclei of all epidermal layers

(Fig. 6) [38]. The most promising technologies resulting from the consortium evaluation were microneedles [22, 39], including steel and dissolvable, which mechanically pierce through the stratum corneum outer barrier and deposit the siRNA cargo in the live skin layers. Following completion of that study, we reported the ability of a motorized microneedle array system to also deliver functional siRNA to skin and inhibit expression in the same mouse model [34]. This is an excellent demonstration of a combination of

Table 2
Published technologies for delivery of functional siRNA to skin

Delivery methodology	Targeted gene	% Target inhibition	Model system	References
Intradermal injection				
Hypodermic needle	EGFP/fLuc	97[a]	Mouse footpad skin	[47]
ID injection/ electroporation	COX-1	51	Atopic dermatitis mouse model	[48]
Topical formulations				
Aquaphor/PG	Luc2p	48	PPK reporter transgenic mouse	[42]
GeneCream	Osteopontin	89	Rheumatoid arthritis mouse model	[41]
Cream-based ointment	CD86	80	Mouse ear skin	[49]
SNA nanoparticles	EGFR	65/75	Mouse skin/human skin equivalent	[46]
Microneedles				
Steel	hMGFP/CBL	29	Skin reporter transgenic mouse	[39]
Dissolvable (PAD)	hMGFP/CBL	50	Skin reporter transgenic mouse	[38]
Dissolvable (PAD)	CD44	52	Human skin grafted on mouse flank	[50]
Motorized (MMNA)	hMGFP/CBL	78	Skin reporter transgenic mouse	[34]
Penetrating peptides				
SPACE peptide	IL-10/GAPDH	28/42	Mouse skin	[44]
SPACE/DOTAP	GAPDH	63	Mouse skin	[45]
TD1-R8 peptide cream	MITF	52	Mouse skin	[43]
TD-1 peptide	GAPDH	51	Rat footpad skin	[51]

[a]Target gene and siRNA were co-delivered

approaches, the motorized microneedle array, a physical method for crossing the stratum corneum, and a chemical approach in which the siRNA is modified to improve delivery across the cell membrane—these are called self-delivery siRNAs (sd-siRNA).

A number of research groups have also reported the ability of topical formulations to deliver functional siRNA to skin (Table 2). In a mouse rheumatoid arthritis model, Takanashi et al. were able to achieve dermal and subdermal siRNA delivery with a topical cream formulation and inhibit osteopontin mRNA levels, preventing irreversible damage to cartilage and bone [41]. Using a modified Aquaphor/propylene glycol (PG) formulation containing high levels of siRNA (approximately 10 μM), Hegde and coworkers

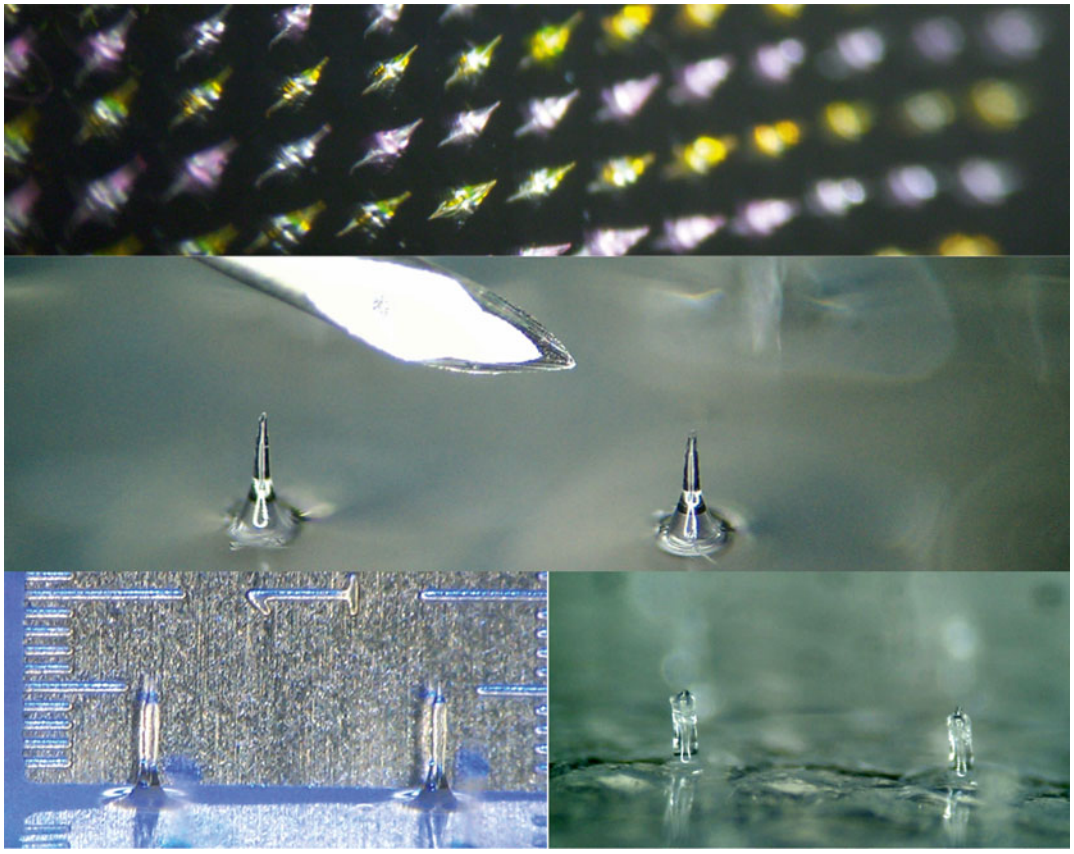

Fig. 6 Soluble polyvinyl alcohol (PVA) microneedles. *Top panel*. Microneedle array showing alternate row loading of fluorescently labeled siRNA mimics. *Middle*. 36 G stainless hypodermic needle vs. microneedle dimensions. *Lower left*. 600 μm microneedles shown against a micro ruler. *Lower right*. Erosion of top portion of microneedles is observed after skin application

inhibited luciferase expression in a palmoplantar skin reporter mouse [42]. A number of groups have used peptides to facilitate stratum corneum penetration and cellular uptake, with one of them Yi et al. [43], moving to human use to treat melasma. Indeed, this technology has now been approved in China as a cosmetic product (www.biomics.cn/en/br1.htm). The Mitragotri laboratory has used a proprietary Skin Permeating And Cell Entering (SPACE) peptide alone [44] or with DOTAP [45] to topically deliver siRNA to skin. As a final example, the Mirkin and Paller groups have demonstrated that spherical nucleic acid (SNA) nanoparticles, initially formed around gold particles but subsequently manufactured without, can deliver siRNA to mouse skin and human skin equivalents [46].

2 Materials

2.1 In Vivo Bioluminescence Imaging

1. Low light imaging system such as an IVIS (Perkin Elmer; previously CRi Inc., Woburn, MA).
2. Substrates:
   (a) Luciferin (Biosynth, International, Inc., Naperville, IL, cat. no. L-8220; 1 g). Stock concentration 30 mg/mL in PBS, aliquot, and store at −20 °C.
   (b) Coelenterazine (Nanolight, cat. no. NFCTZFB; 5 mg). Stock concentration 10 mg/mL in ethanol, aliquot, and store at −80 °C. For working stock, dilute frozen stock 10 μL into 1.5 mL of PBS (working stock concentration 67 μg/mL). Do not store.
3. Anesthetic agent (e.g., isoflurane at 2–3 %).

2.2 In Vivo Fluorescence Imaging

1. Low light imaging system such as an IVIS or Maestro or intravital microscope such as the Caliber ID VivaScope 2500 (formerly Lucid Inc., Rochester, NY).
2. Anesthetic agent (e.g., isofluorane at 2–3 %).
3. Aquasonic® 100 ultrasound transmission gel (Parker laboratories, INC. Fairfield, NJ).
4. Crodamol™ STS as index matching fluid (Croda Inc., Edison, NJ).

2.3 Plasmid Expression Constructs [22, 33]

1. Reporter gene plasmids—multifunctional (Fig. 7).
   (a) pTD138—hMGFP/CBL driven by the CMV immediate early promoter.
   (b) pTD166—Luc2/eGFP driven by the ubiquitin C (UbiC) promoter.
   (c) pTD239—K6a(wt)/eGFP driven by the CMV promoter.
   (d) pTD240—K6a(N171K)/eGFP driven by the CMV promoter.
   (e) pTD128—K6a(wt)/tdTFP driven by the CMV promoter.
   (f) pTD129—K6a(N171K)/tdTFP driven by the CMV promoter.
   (g) pTD241—K6a(wt)/eGFP driven by the UBC promoter.
   (h) pTD242—K6a(N171K)/eGFP driven by the UBC promoter.
   (i) pTD202—K6a(wt)/tdTFP driven by the UBC promoter.
   (j) pTD203—K6a(N171K)/tdTFP driven by the UBC promoter.

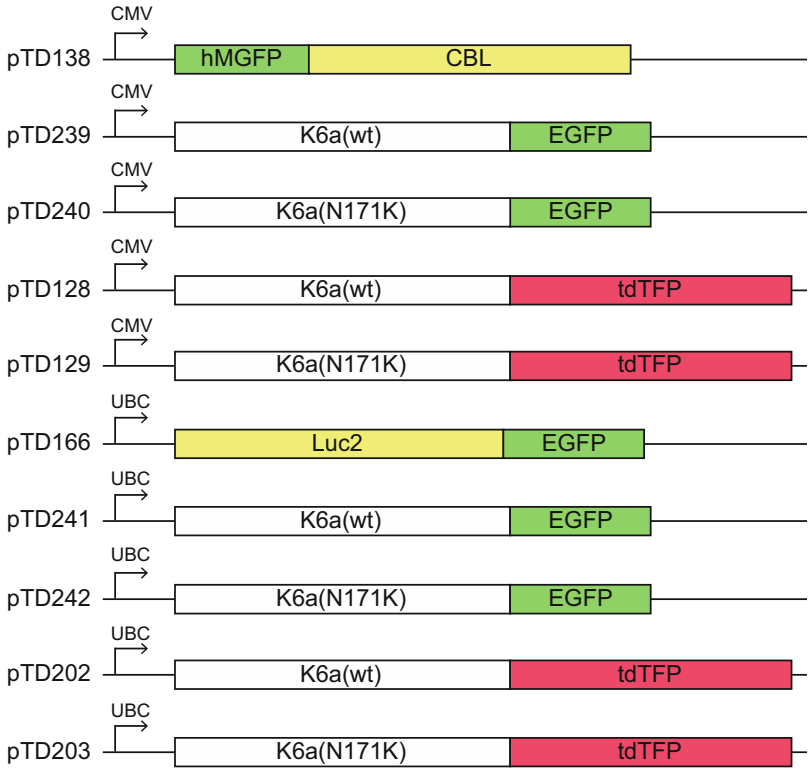

Fig. 7 Schematic representation of expression plasmids used for in vivo fluorescence and bioluminescence imaging of reporter proteins

2.4 siRNAs (Unmodified and Accell-Modified) [16, 22, 33] Were Provided by Dharmacon Products GE Healthcare (Lafayette, CO)

1. CBL3 siRNA (targets the dual function reporter construct in the RLG reporter mouse and pTD138).
   Sense: 5′-UUUACGUCGUGGAUCGUUAuu.
   Antisense: 5′-P-UAACGAUCCACGACGUAAAuu.
2. K6a_513a.12 siRNA [7] (targets the human keratin 6a N171K mutant allele containing a single point mutation in plasmids pTD240, pTD129, pTD242, and pTD203; wt plasmids pTD239, pTD128, pTD241, and pTD202 are used as controls; see Notes for design).
   Sense: 5′-CCCUCAAaAACAAGUUUGCuu.
   Antisense: 5′-P-GCAAACUUGUUUUUGAGGGuu.
3. K6a_3′UTR.1 (targets the 3′ UTR of K6a).
   Sense: 5′-GCACAAGUGACUAGUCCUAuu.
   Antisense: 5′-P-GCAAACUUGUUUUUGAGGGuu.
4. CD44 siRNA (targets exon 1 of CD44).
   Sense: 5′-GGCGCAGAUCGAUUUGAAUuu.
   Antisense: 5′-P-AUUCAAAUCGAUCUGCGCC.

5. NSC4 siRNA (targets inverted betagalactosidase sequence).
   Sense: 5′-UAGCGACUAAACACAUCAAuu.
   Antisense: 5′-P-UUGAUGUGUUUAGUCGCUAuu.
6. Unmodified eGFP siRNA (or Accell modified).
   Sense: 5′-GCACCAUCUUCUUCAAGGAuu.
   Antisense: 5′-P-UCCUUGAAGAAGAUGGUGCuu.
7. An siRNA of your choosing.

2.5 Plasmid DNA Injections

1. A 1 mL syringe with a 28-G needle is used to deliver 50–75 μL of plasmid solution intradermally to mouse footpads. A bleb is formed if the injection is performed properly. Note that large volumes are needed to generate pressure, which facilitates nucleic acid delivery to keratinocytes [15].
2. Endotoxin-free plasmids encoding reporter genes expressed from strong constitutive mammalian promoters (*see* Subheading 2.3).

2.6 Meso-Assisted Delivery of sd-siRNA

1. A Motorized Meso Machine (Triple-M from Bomtech Electronics Co., Seoul, Korea) [34].

2.7 Generation and Evaluation of Human Skin Equivalents

1. Epidermal skin equivalents [2].
2. Full thickness skin equivalents grafted onto immunocompromised mice.
   (a) Humanized mouse model [50].
   (b) Pachyonychia congenita humanized disease mouse model [52].

2.8 In Vivo Confocal Microscopy with the VivaScope or DAC Microscopes

1. Caliber ID VivaScope 2500 System [22].
2. Alternatively a DAC microscope could be used [30].
3. Aquasonic® 100 ultrasound transmission gel (Parker laboratories, INC. Fairfield, NJ).
4. Crodamol™ STS as index matching fluid.
5. Amira® software (Visage Imaging, Carlsbad, CA).

3 Methods

3.1 Plasmid Delivery Models of Gene Silencing

Plasmids encoding reporter genes can be used as the target for siRNA therapy or as a means of assessing nucleic acid transfer to tissues. There are a wide variety of plasmids encoding single and combination reporter genes (Fig. 7). Each of these could be used to evaluate siRNA gene silencing provided that an siRNA has been developed and tested for that specific reporter gene sequence.

1. Inject the reporter plasmid into the footpad skin of anesthetized Swiss Webster mice at concentrations of 10–20 μg of DNA in 50–75 μL PBS intradermally using a 1 mL insulin

syringe. 60–80 μg (4.5 nmol) of the siRNA could be mixed with the plasmid, or alternatively the siRNA could be injected separately [24]. The siRNA can be used alone or in combination with pUC19 (5 μg) as a "carrier" nucleic acid. The positive control for experimental gene delivery tools can be direct intradermal injection (10–20 daily injections of 60–80 μg per treatment) of specific CBL3 siRNA into the control footpad of white mice with reporter expression in the skin. Use an equal amount of irrelevant siRNA (K6a_513a.12) as a negative control injected intradermally into the contralateral footpad.

2. If the siRNA is to be injected separately, load the syringe with CBL3 siRNA (or siRNA of choice) and inject at 60–80 μg (4.5 nanomoles) per footpad in 50–75 μL PBS alone or in combination with pUC19 (5 μg) as a potential "carrier" [47] and at the site of plasmid injection.
3. Set up the control with an equivalent quantity of irrelevant siRNA (e.g., K6a_513a.12) [7] and inject intradermally into the counterpart footpad.
4. Follow gene expression using in vivo bioluminescence or fluorescence imaging as determined by the reporter gene used.

3.2 Testing of siRNA in Human Skin Equivalents in Mice

1. Full-thickness 3-D human skin equivalents can be obtained from a commercial source or prepared by a variety of methods whereby keratinocytes are embedded in a matrix of fibroblasts and cultured to generate a 3-D human skin equivalent (*see* Garcia et al. [52] for an example).
2. Graft human skin equivalent on to an anesthetized immunocompromised mouse by inserting a square region (2 × 2 cm) of skin equivalent into the back of the mouse (mouse skin previously removed) carefully aligning both mouse and human skin [22]. Cover the grafted area with Vaseline gauze and bandages and leave the dressing for 14 days.
3. Administer siRNA to the human skin equivalents (ID injection, microneedle arrays, etc.) about 1–2 month after the skin graft procedure. Microneedle application methods vary depending on the type of microneedle array, and can include manual application using forceps (steel microneedles) or by finger flicking, vacuum or spring-loaded application devices for application of dissolvable microneedle arrays [50].
4. Monitor gene expression using in vivo bioluminescence or fluorescence imaging as determined by the reporter gene used.
5. Harvest skin and prepare for histologic examination [50].

3.3 In Vivo Bioluminescence Imaging (BLI)

1. Anesthetize mice with 2–3 % isoflurane.
    1. Inject 100 μL of d-luciferin (Biosynth) at a concentration of 30 mg/mL solution (~150 mg/kg body weight) into the peritoneal cavity of mice under isoflurane anesthesia.

2. Wait 10 min for the luciferin to distribute throughout the body of the mouse.
3. Image live anesthetized mice using the IVIS Spectrum Imaging System (Xenogen product from Caliper LifeSciences, Alameda, CA) [53] or equivalent device.
4. Quantify light emission using LivingImage software 3.1 (Caliper LifeSciences, Alameda, CA).

3.4 Fluorescence Imaging with the VivaScope 2500 [21, 33]

1. Anesthetize mice with 2–3 % isoflurane.
2. Apply Aquasonic® 100 ultrasound transmission gel, as an immersion medium, between the objective lens of the Calilber ID VivaScope 2500 System and the glass window of the tissue cassette [21, 33].
3. Place the mouse paw to be imaged over the glass window of the tissue cassette after adding Crodamol™ STS as index matching fluid (index of refraction = 1.47).
4. Image GFP and/or RFP reporter expression in paws using the Calilber ID VivaScope 2500 [21, 33].
5. Adjust the z-depth position of the VivaScope by identifying the surface of the tissue using the 658 nm reflectance laser. Using this same laser, the position in the skin (e.g., stratum corneum, granulosum, spinal layer, basal layer) can be identified [54].
6. After switching to the 488 nm fluorescence excitation laser, generate VivaBlocks (*xy* position map) to screen the tissue to locate GFP-positive cells (the signal displays as white colored over a black background) at the selected depth.
7. Once cells expressing eGFP or hMGFP are found, generate VivaStack (*z*-axis map) images, first in fluorescence mode, and then in reflectance mode (40 slices with a *z* separation of 1.6–8 μm between slices. The field of view is 750 × 750 μm and the images are collected at nine frames per second. Image files are processed and 3-D volumes and video files reconstructed using ImageJ (National Institutes of Health, Bethesda, MD).
8. Can be repeated with the 532 nm fluorescence excitation laser to capture red (e.g., tdTFP reporter expression) fluorescence.

3.5 Intravital Microscopy with the DAC Microscope

1. Perform intravital imaging on anesthetized mice. Use isoflurane anesthesia, or alternative anesthetic following institutional guidelines.
2. Use optical gel (NyoGel® OC-431A-LVP, Nye Lubricants Inc., Fairhaven, MA, index of refraction = 1.46) as a coupling agent between the footpad skin and the microscope.
3. Analyze the footpads by intravital imaging at various timepoints during and after treatment using a DAC microscope equipped with a fiber-coupled 488 nm wavelength laser [27].

4. Scan the footpads at a single depth of ~20 μm to localize both those regions expressing EGFP or hMGFP and those where the signals were absent.
5. Once the signal is found, collect image stacks at these sites.
6. Process and reconstruct the stacks into volumes and video files using Amira® software [30].

3.6 Image Processing

1. Export VivaScope native grayscale image stacks as TIF images for processing using NIH ImageJ and FIJI public domain image-processing software.
2. Image stacks can be despeckled to remove outlier noise pixels, processed with an unsharp mask filter algorithm (Sigma = 1.0, Weight = 0.7), and false-colored in the case of fluorescence data.
3. Image intensity distributions (window and level) can be set to common standard values across respective image sets to normalize intensities for comparison.
4. 3-D representations can be derived from these data (Fig. 8).

3.7 In Vivo Fluorescence Imaging with Wide Field System

1. Anesthetize mice with isoflurane and image using the Maestro Optical imaging system or IVIS imaging system if equipped with spectral unmixing capabilities as previously described [55].
2. Acquire images with an excitation filter of 445–490 nm and a long-pass emission filter (515 nm).
3. Capture Images at 10 nm windows from 500 to 700 nm using the Maestro software (exposure times are automatically calculated).

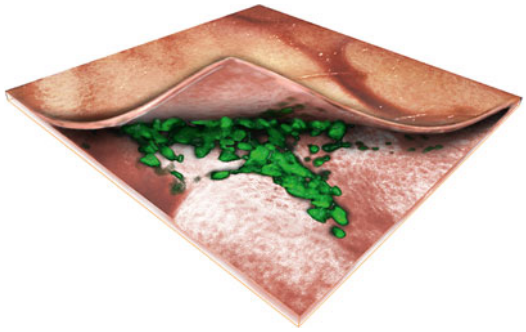

Fig. 8 A virtual peeled-back representation of noninvasive visualization of reporter expression in keratinocytes of mouse skin. This stylized representation of EGFP reporter expression was used to demonstrate imaging of EGFP expression in mouse skin. An EGFP expression plasmid was injected intradermally into a mouse footpad. At 36 h after injection, the footpad of the living mouse was imaged noninvasively with the VivaScope as described in Fig. 1. The colorized stacks corresponding to EGFP (*green*) and reflectance (total skin morphology, skin tones) were manipulated using Editable Poly with a Bend modifier (3ds Max, Auto Desk) to represent the ability to noninvasively image and monitor reporter gene expression beneath the skin surface

4. Use spectral unmixing of the resulting cube images with a user-defined GFP protocol.
5. Set the spectrum manually by unmixing autofluorescence from a negative non-hMGFP expressing mouse analyzed in parallel with a Tg CBL/hMGFP positive mouse.
6. Draw regions of interest around the palm of each paw and calculate the average signal (counts/s/mm^2).
7. Calculate the ratio of average signals in right (CBL3) versus left (nonspecific control) paws for each mouse and normalize with respect to the pretreatment analysis data.
8. For presentation, the unmixed GFP signal can be pseudo-colored green, etc.

3.8 Histological Analysis of Fluorescently Labeled sd-siRNA Distribution in Murine and Human Skin to Validate In Vivo Images

1. After sacrificing of the mouse remove the skin tissues from the footpad.
2. For cryosections, embed skin in OCT compound and freeze directly on dry ice.
3. Cut vertical section at 10 μm.
4. Mount sections with Hydromount™ (National Diagnostic, Highland Park, NJ) containing DAPI for nuclear staining.
5. Image sections using a Zeiss Axio Observer Inverted Fluorescence Microscope equipped with Cy3 and DAPI filter sets, or equivalent microscope.
6. Stitch images together using Microsoft Image Composite Editor (ICE).

3.9 Plasmid Delivery via Dissolvable Microneedle Arrays

1. Coat microneedle (also known as protrusion array devices, PAD [38]) arrays (3 × 5 needles per array), with pUbc-luc2/eGFP or pCMV-hMGFP/CBL expression plasmids.
2. Flick the array with a finger to seat the needle tips into the paw and hold the PAD in contact with the skin for 1 min.
3. Apply control PADs, loaded with β-gal expression plasmid DNA (pCMVsport-β-gal, Invitrogen), to the contralateral paws.
4. After removal, PAD arrays can be observed under an inspection Amscope SM1-BZ microscope (Iscope Corp, Chino, CA) to assess skin penetration and needle dissolution (Fig. 6). In our hands, the post-insertion inspection of the array confirmed penetration of ~5 needles per array per application, as determined by the absence of a tip at the end of the needle due to dissolution upon insertion and removal.
5. Treated paws can be analyzed by in vivo bioluminescence imaging, fluorescence imaging using the VivaScope system or by traditional microscopy of frozen skin sections.

3.10 Plasmid Delivery via Steel Microneedle Arrays

1. Coat metal microneedle arrays (1 × 5 needles per array) with pUbc-luc2/eGFP or pCMV-hMGFP/CBL.
2. Hold the coated arrays tightly with a forceps and insert the array into the skin of the paw by pushing until full penetration is achieved.
3. As a negative control, treat the contralateral paw of each with metal microneedle arrays coated with salmon sperm or other non-coding DNA.
4. Leave the arrays seated in the skin for 20 min to give the DNA payloads the opportunity to dissolve inside the skin.
5. Treated paws can be analyzed by in vivo bioluminescence imaging, fluorescence imaging using the VivaScope system or by traditional microscopy of frozen skin sections.

3.11 Evaluating the Arrays in Human Skin Equivalents

1. Apply PAD arrays (5 × 5 microneedles) to human skin equivalents [50] using a vacuum channel plate made from a modified 0.2 μm sterile syringe filter (Whatman, Florham Park, NJ), with one face and filter removed, leaving a channeled plate with an exhaust port. The vacuum is an alternative to flicking the array as mentioned above or spring-loaded application.
2. Attach the exhaust port to a vacuum pressure station (Bernant Company, Barrington, IL) providing a stable flat surface with sufficient airflow to hold a PAD over the skin surface.
3. Upon contact with the plate, seat the mouse skin immediately against the channeled plate and then insert the needles into the skin.
4. Continue the vacuum for 1 min and then remove the channeled plate.
5. Leave PADs for 20 min in the skin to allow needle dissolution and then remove the PAD.
6. Coated metal microneedles can be applied to human skin equivalents in a similar fashion as described above for mouse paws.

3.12 Meso-Assisted Delivery of sd-siRNA to Mouse and Human Skin Using a MOTORIZED Meso Machine (Triple-M) [34]

1. Load unlabeled or labeled siRNA of interest such as Cy3-Accell Non-Targeting siRNA (Dharmacon Products) into the chamber of the disposable Meso needle cartridge of the Meso device (50–300 μL at 0.1 mg/mL).
2. Set the device to a depth of 0.1 mm.
3. Lay a fold of skin on a rigid support positioned under the tip of the Meso device. Once the Meso device is oriented vertically and is perpendicular to the fold of skin, turn on the device set at the highest speed and hold in place for 10 s.
4. To treat fresh human abdominal skin (obtained immediately following surgical procedures), manually stretch and pin the skin to a cork platform and treat was with mouse skin (above).

5. Image with an IVIS Lumina imaging system, or equivalent, using the 535 nm excitation and DsRed emissions settings (1–10 s acquisition time).
6. Quantify the data using LivingImage software (Perkin Elmer).
7. Subtract the fluorescent background from an untreated area of the same animal or tissue sample and report values reported as radiant efficiency.
8. Present pseudocolored image as an overlay over the grayscale reference image.

3.13 Meso-Assisted Delivery of sd-siRNAs and Analysis of Gene Silencing [34]

1. Anesthetize hairless (SKH1) tg-CBL/hMGFP mice and treat, every other day, with 100 μL of 5 mg/mL solution in PBS of either CBL3 sd-siRNA or a nonspecific control sd-siRNA (CD44 or TD101) for 11 days (six treatments total).
2. On the day following the last treatment (day 12), sacrifice the mice and excise the treated areas and analyze by both fluorescence microscopy and RTqPCR as described in [33].
3. For RTqPCR, separate the epidermis from the dermis by incubation in dispase II (Roche, Indianapolis, IN, 10 mg/mL in PBS) for 2–4 h at 21 °C prior to RNA isolation from the epidermis only.

3.14 Flourescent Triplex-Forming Molecules

1. AG30 has the sequence AGGAAGGGGGGGGTGGTGGG GGAGGGGGAG and binds to the polypurine target at positions 167–196 of *supFG1*. It was synthesized by Midland Certified reagent Company (Midland, TX) with a 3′-propylamine and FITC at the 5′ end [23, 56].
2. PNA-Antp has the sequence, JJJJJTTJJT-O-O-O-TCCTTCCCCC-O-O-KKKKKWKMRRNQFWIKIQR, where J = pseudoisocytosine and O = 8-amino-2,6,dioxaoctanoic acid. It was designed to bind as a clamp to the homopurine strand of positions 167–176 of *supFG1*. The cell penetrating peptide, antennapedia, was covalently linked to the PNA at the C-terminal lysine. FITC was conjugated to the PNA at the N-terminus via two O linkers.
3. The AV *supFG1* mice were derived in a CD1 background as described [56] and bred into the SKH hairless background [23].
4. Inject 10 μg FITC-PNA-Antp in 50 μL PBS into the tail dermis of SKH *supFG1* transgenic mice [23].
5. Prepare stratum corneum-stripped skin by sequential application and removal of d-Squame (CUDERM Co., Dallas, TX) tapes followed by a cyanoacrylate strip, in which a drop of cyanoacrylate is placed on a glass slide, inverted onto the mouse skin for 1 min and then remove quickly.
6. Apply FITC-AG30, 200 ng in 2.5 μL PBS, to 1 cm^2 of stratum corneum-stripped back skin and allow to dry.

4 Conclusions

Despite the accessibility of the skin, the barriers to nucleic acid delivery remain formidable. Imaging can be used to accelerate the study of various topical delivery methods and the images from these studies have served to inform and guide the development of new tools. Skin delivery of nucleic acids and functional delivery are distinct, and imaging has illustrated this clearly. Through the use of reporter genes that reveal the effects of a nucleic acid on the biology of the cell, we can appreciate the accomplishments in this field, and yet, they highlight the significant challenges in the creation of clinically viable transdermal gene delivery tools for treating human disease.

Acknowledgments

This work was funded in part by the NIH through a grant called the NIH NIAMS GO Delivery! consortium grant (to RLK, LMM and CHC; RC2AR058955), support from the Pachyonychia Congenita Project (RK and CHC), and a gift from the Chambers Family Foundation (CHC).

References

1. Lorenzer C et al (2015) Going beyond the liver: progress and challenges of targeted delivery of siRNA therapeutics. J Control Release 203:1–15
2. Hickerson RP et al (2011) Use of self-delivery siRNAs to inhibit gene expression in an organotypic pachyonychia congenita model. J Invest Dermatol 131:1037–1044, In press
3. Leachman SA et al (2008) Therapeutic siRNAs for dominant genetic skin disorders including pachyonychia congenita. J Dermatol Sci 51(3):151–157
4. Leachman SA et al (2010) First-in-human mutation-targeted siRNA phase Ib trial of an inherited skin disorder. Mol Ther 18(2):442–446
5. Leslie Pedrioli DM et al (2012) Generic and personalized RNAi-based therapeutics for a dominant-negative epidermal fragility disorder. J Invest Dermatol 132(6):1627–1635
6. Préat V, Dujardin N (2001) Topical delivery of nucleic acids in the skin. STP Pharma Sci 1:57–68
7. Hickerson RP et al (2008) Single-nucleotide-specific siRNA targeting in a dominant-negative skin model. J Invest Dermatol 128(3):594–605
8. Wong P, Domergue R, Coulombe PA (2005) Overcoming functional redundancy to elicit pachyonychia congenita-like nail lesions in transgenic mice. Mol Cell Biol 25(1):197–205
9. Smith FJ et al (2008) Development of therapeutic siRNAs for pachyonychia congenita. J Invest Dermatol 128(1):50–58
10. Chen J, Roop DR (2005) Mouse models in preclinical studies for pachyonychia congenita. J Investig Dermatol Symp Proc 10(1):37–46
11. Cao T et al (2001) An inducible mouse model for epidermolysis bullosa simplex: implications for gene therapy. J Cell Biol 152(3):651–656
12. Broderick KE, Humeau LM (2015) Electroporation-enhanced delivery of nucleic acid vaccines. Expert Rev Vaccines 14(2):195–204
13. Vogel FR, Sarver N (1995) Nucleic acid vaccines. Clin Microbiol Rev 8(3):406–410
14. Colluru VT et al (2013) Preclinical and clinical development of DNA vaccines for prostrate cancer. Urol Oncol. doi:10.1016/j.urolonc.2013.09.014, Pii: S1078-1439(13)00387-6
15. Gonzalez-Gonzalez E et al (2010) Increased interstitial pressure improves nucleic acid deliv-